Military Technical College
Kobry Elkobbah,
Cairo, Egypt

2nd International Conference
on Electrical Engineering
ICEENG 99

DESIGN OF INFRARED THERMOGRAPHIC SYSTEM FOR POSITIONING AND COORDINATION

Elfallal* I. A.; Saad S. M. S.; Elmehrez*** N. H.**

ABSTRACT

Thermography and spectroradiometry are very strong tools for night vision and target detection. Starers and scanners were normally used for imaging of targets without the existence of a facility to locate these targets. An imaging technique in which the determination of targets location is presented. In this design of the imaging system, the frequency-modulated reticle was used instead of the chopper. Through the method of arc length differentiation, after demodulation, the output signal is obtained. The analysis showed that the design was strongly dependent on geometrical parameters instead of time. Using the point model results to analyze the parameters of the designed system, the imaging system can be used to locate the targets. In this work, a case study was presented and analyzed, to show how the thermographic system can be used for target coordination.

KEY WORDS: thermographic system; imaging; starers; scanners.

---

* Asst. Prof. – Egyptian Armed Forces.
** Asst. Prof. - Egyptian Armed Forces.
*** Syrian Armed Forces.

1. INTRODUCTION

Infrared imaging [1], or thermography, is the acquisition of infrared radiation due to the distribution of heat in object space and the variation of this distribution in time. The imaging system must transfer the infrared radiation into a visible image. To suppress unwanted signals from backgrounds, the basic concept is to use a chopper. The chief function of the chopper is to provide an alternating or pulsed form of radiation into a detector [2].

Thermal imaging systems have the disadvantage of detection of radiation sources that is not accompanied by the determination of their coordinates, i.e., it cannot identify the targets position. A glance idea is to use a reticle instead of the chopper.

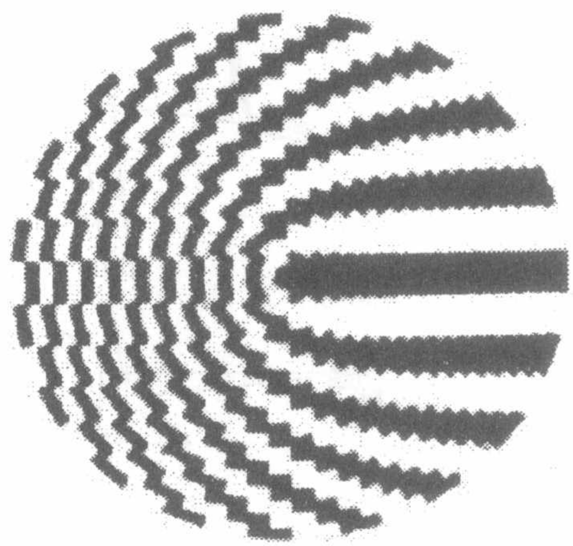

Fig. 1. Discrete frequency versus radius FM reticle

Reticles have been studied as a means of providing target information for tracking system [3-10]. Effective methods for characterizing the transmission function of an amplitude-modulated reticle [11] and a frequency-modulated (FM) reticle were developed by Driggers [12]. One particular type of FM reticle is the frequency versus radius binary reticle (Fig. 1). Driggers et. al. showed that this reticle could be used for IR imaging system [13], and therefore this paper, will follow his procedures and generalize its use with thermography.

A common way to construct an FM reticle is to let the light beam nutate around the axis, with the reticle stationary [7]. Figure 2 shows the configuration of such a system. Radiation from the scene enters through the optics. The image is scanned vertically and horizontally, directing the rays to the mirror, which is mounted with a slight tilt, and focused to form a spot in plane, where a stationary reticle is put.

The rotation of the mirror causes the beam, and hence the spot, to nutate. The rays then travel through the reticle, becoming frequency modulated, and falls onto the detector. The output signal V_s of the detector is also frequency modulated and is sent to the discriminator, which electronically demodulates the signal to yield a final output signal u, which is used to perform the aiming function (target coordination).

In this paper we present the point model and the mathematical modeling on which the processing software is based. Also, a few case studies are presented.

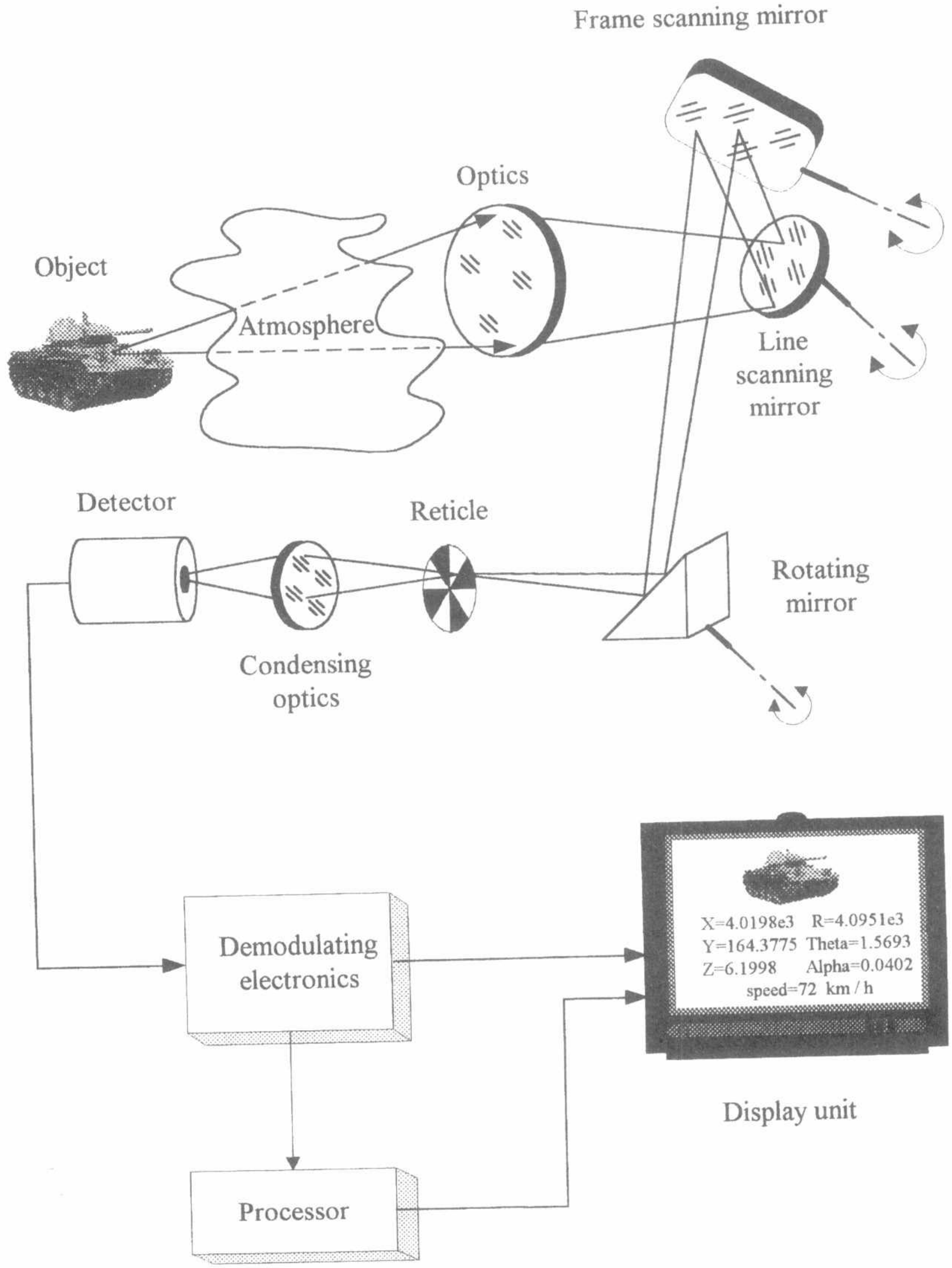

Fig. 2. system component diagram

2. ANALYSIS

2.1 Point Model

Assuming that the image spot is an ideal point. Figure 3 shows that the image point P nutates with a constant angular velocity ω along a circular loop of radius a around the center O_1, which in general does not coincide with the reticle center O. In system O-Y-Z, the polar coordinates of O_1 and P are (r_1, θ_1) and (ρ, θ), respectively

The transmission of reticle shown in Fig. 3 is given by [13]:

$$\tau_r(r,\theta) = \frac{1}{2} + \frac{1}{2}\operatorname{sgn}(\cos[\, m(a)\,\theta\,]) \tag{1}$$

where the signum (sgn) function is equal to –1 when its argument is < 0 and is equal to 1 when its argument is ≥ 0, and $m(a)$ is one-to-one frequency versus radius parameter, and it for this transmission equation is

$$m(a) = 20\frac{a}{R} \tag{2}$$

where R is the radius of the reticle.

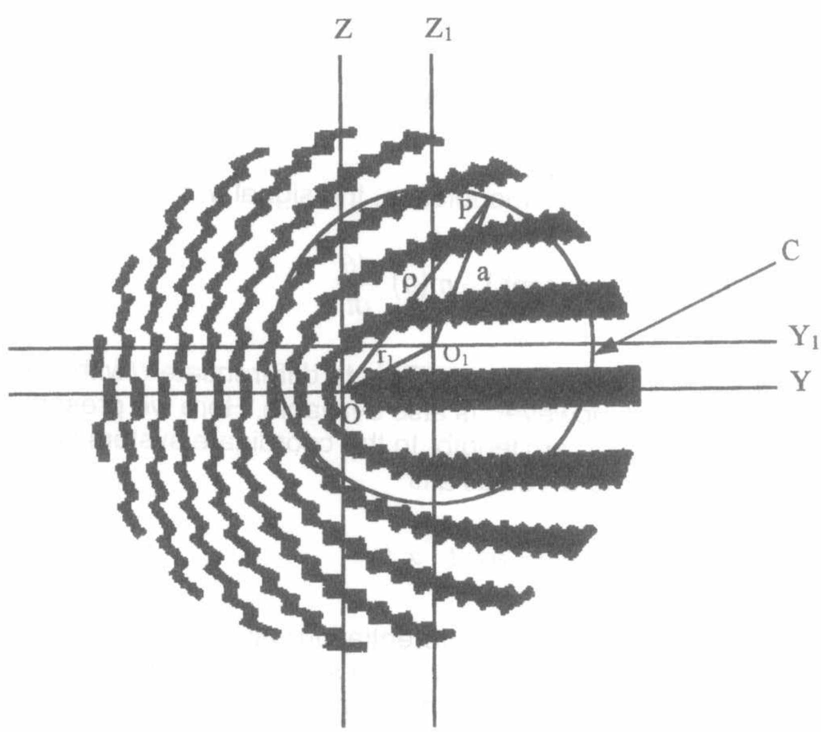

Fig. 3. Discrete $m(r)$ FM reticle-point model

To derive an expression for the signals *v* and *u* let us proceed as follows: The detector output voltage is proportional to the total radiation behind the reticle, which is given by [7]:

$$v(t)=\iint_{-\infty}^{\infty} f(x,t)p_I(x,t)d^2x \tag{3}$$

where $f(x,t)$ is the transmittance function of the reticle and $p_I(x,t)$ is the distribution function of the image. Now the image is a point, the function *p* can be written as:

$$p_I(x,t)=\delta[y-y'(t)]\,\delta[z-z'(t)] \tag{4}$$

where $y'(t)$ and $z'(t)$ are the instantaneous positional coordinates of the image point. For the function $f(x,t)$, notice that the reticle is stationary, so $f(x,t)=f(x)=\tau_r(r,\theta)$. Hence, using eq. (1), we have

$$f(x)=\frac{1}{2}+\frac{1}{2}\operatorname{sgn}(\cos[m(a)\,\theta\,]) \tag{5}$$

Substituting egs. (5) and (4) into eq. (3), we get

$$v(t)=\int_{-\infty}^{\infty}\int_{-\infty}^{\infty}\left\{\frac{1}{2}+\frac{1}{2}\operatorname{sgn}(\cos[m(a)\,\theta\,])\right\}\delta(y-y')\delta(z-z')dy\,dz$$

$$=\frac{1}{2}+\frac{1}{2}\operatorname{sgn}(\cos[m(a)\,\theta\,])$$

$$v(t)=\frac{1}{2}+\frac{1}{2}\operatorname{sgn}[\cos(\text{argument})] \tag{6}$$

According to the definition of FM demodulation, the signal *u* is

$$u(t)=\frac{d}{dt}(\text{argument})=m(a)\,\frac{d\theta}{dt} \tag{7}$$

A straightforward way to work out eq. (7) is to differentiate θ with respect to *t*, the time [14]. Another method, however, is also available. Here we present a method of differentiation with respect to arc length. In the coordinate system O_1-Y_1-Z_1, the arc length *s* along the circular loop of radius *a* is

$$s=\int a\,(\omega\, dt)=a\,\omega\, t\ \ \propto t \tag{8}$$

Since *s* is proportional to *t*, the differentiation with respect to *t* in eq. (7) can be replaced by the differentiation with respect to *s*. Transforming to system O-Y-Z, we have the expression for arc length in another form:

$$s=\int_0^{\theta}\rho\, d\theta-c$$

$$s=\int_0^{\theta}\left[r_1\cos(\theta-\theta_1)+\sqrt{a^2-r_1^2\sin^2(\theta-\theta_1)}\right]d\theta-c$$
$$=r_1\sin(\theta-\theta_1)+r_1\sin\theta_1+a\left\{(\theta-\theta_1)\left[1-\frac{1}{4}k^2-\frac{3}{64}k^4-\frac{5}{256}k^6+\cdots\right]\right.$$
$$+\sin(\theta-\theta_1)\cos(\theta-\theta_1)\left[\frac{1}{4}k^2+\frac{1}{32}k^4\sin^2(\theta-\theta_1)+\frac{3}{64}k^6\right.$$
$$\left.\left.+\frac{1}{96}k^6\sin^4(\theta-\theta_1)+\frac{5}{384}k^6\sin^2(\theta-\theta_1)+\frac{5}{256}k^6+\cdots\right]\right\}$$
$$-a\sin^{-1}\left(\frac{r_1}{a}\sin\theta_1\right) \qquad (9)$$

where

$$c=a\sin^{-1}\left(\frac{r_1}{a}\sin\theta_1\right)$$
$$k=\frac{r_1}{a}$$

Differentiation of s with respect to θ gives

$$\frac{ds}{d\theta}=r_1\cos(\theta-\theta_1)+a\left\{\left(1-\frac{1}{4}k^2-\frac{3}{64}k^4-\frac{5}{256}k^6+\cdots\right)\right.$$
$$+\cos 2(\theta-\theta_1)\left[\frac{1}{4}k^2+\frac{3}{64}k^4+\frac{5}{256}k^6+\cdots\right]$$
$$+\left[3\sin^2(\theta-\theta_1)\cos^2(\theta-\theta_1)-\sin^4(\theta-\theta_1)\right]\left(\frac{1}{32}k^4+\frac{5}{384}k^6+\cdots\right)$$
$$\left.+\left[5\sin^4(\theta-\theta_1)\cos^2(\theta-\theta_1)-\sin^6(\theta-\theta_1)\right]\left(\frac{1}{96}k^6+\cdots\right)\right\} \qquad (10)$$

Substituting eqs. (8) and (10) into eq. (7), we have

$$u(\theta)=m(a)\,a\omega\,\frac{1}{\frac{ds}{d\theta}}$$
$$u(\theta)\approx m(a)\,a\omega\left\{r_1\cos(\theta-\theta_1)+a\left(1-\frac{1}{4}k^2-\frac{3}{64}k^4-\frac{5}{256}k^6+\cdots\right)\right.$$
$$+a\cos 2(\theta-\theta_1)\left[\frac{1}{4}k^2+\frac{3}{64}k^4+\frac{5}{256}k^6\right]$$
$$+a\left[3\sin^2(\theta-\theta_1)\cos^2(\theta-\theta_1)-\sin^4(\theta-\theta_1)\right]\left(\frac{1}{32}k^4+\frac{5}{384}k^6\right)$$
$$\left.+a\left[5\sin^4(\theta-\theta_1)\cos^2(\theta-\theta_1)-\sin^6(\theta-\theta_1)\right]\frac{1}{96}k^6\right\}^{-1} \qquad (11)$$

The above formula describes the signal output after demodulation. To verify that this formula really represents a demodulated FM signal, let us consider the simplified case of $k^2 << 1$. We neglect terms higher than k^2 to obtain

$$u(\theta) = m(a)\, a\, \omega \frac{1}{a + r_1 \cos(\theta - \theta_1)}$$
$$= m(a)\, \omega - m(a)\, \omega \frac{r_1}{a} \cos(\theta - \theta_1) \qquad (12)$$

Since θ is a function of t, the above equation can be written in the following form

$$u(t) = u_0 - f(t) \qquad (13)$$

where

$u_0 = m(a)\, \omega$;

$f(t) = m(a)\, \omega \frac{r_1}{a} \cos(\theta - \theta_1)$.

Comparison of this expression with the definition for the instantaneous frequency of a FM signal, i.e., $\varpi = \varpi_0 + f(t)$, reveals that u behaves like a demodulated FM signal.

We can see the usefulness of the method of arc length differentiation. The result that eq. (11) shows is the dependence of u upon θ, not upon t. In other words, instead of being time dependent, the problem has been changed to be geometry dependent.

2.2 Mathematical Modeling

Consider that the target image (the point P) nutates once within a period T. The period T is equal to

$$T = \frac{2\pi}{\omega} \qquad (14)$$

Also, let the circular loop consists of numbers of points, for example 500 points. For each point of the circular loop, eq. (11) gives the value, which characterizes the position of this point with respect to the center of the reticle.

According to Fig. 3, in the coordinate system O_1-Y_1-Z_1, the polar coordinates of the image point P is (ωt, a). So, to find the angle ωt, we need to know the time t when this point starts its circular loop. To discuss that, consider that no target exists in the field of view of the system (FOV) and then suddenly the target appears. When no target exists, the output voltage u is equal to zero. First nonzero voltage value means that the target is in the FOV. Hence, taking the time t at this value, we calculate the angle ωt. Beginning then from this value, we save the voltage values for one period.

We know that in each period there is a maximum value of output voltage. Referring to eq. (12), the maximum value occurs at $\theta - \theta_1 = \pi$, which is given by:

$$u_{\max} = m(a)\omega\left(1 + \frac{r_1}{a}\right) \tag{15}$$

Substituting eq. (2) into eq. (15), we have the radius a

$$a = \frac{u_{\max} R}{20\omega} - r_1 \tag{16}$$

Since we have the polar coordinates of the image point P (ωt, a), we can calculate the Cartesian coordinates, according to Fig. 3, as:

$$\begin{aligned} y_1 &= a\cos\omega t \\ z_1 &= a\sin\omega t \end{aligned} \tag{17}$$

After that, we compare the current voltage values with the saved values. The first finding difference, which means that the target is moved, the time t is taken to calculate the new angle ωt, and then the voltage values for one period is saved to find the peak value for calculating the new radius a. The new angle and the new radius will be used to calculate the new position (y_l, z_l) for the moved target, and so on. If no difference exists between the current voltage values and the saved values, it means that the image point P is nutated twice with the same angle and the same radius around O_1, and thus the target is stationary.

The range to the target can be calculated from the infrared range equation, which is [15]:

$$R_{\text{ran}} = \left[\frac{\pi D_0 (\text{NA}) J \tau_a \tau_0 \tau_r D^*}{2(\Omega \Delta f)^{1/2} (V_s / V_n)}\right]^{1/2} \tag{18}$$

where

- R_{ran} is the range to the target;
- D_0 is the diameter of the entrance aperture of the optics;
- NA is the numerical aperture;
- J is the radiant intensity;
- τ_a is the atmospheric transmitance;
- τ_o is the transmitance of the optics;
- τ_r is the transmitance of the reticle;
- D^* is the detectivity;
- Ω is the instantaneous field of view (IFOV) of the system;
- Δf is the equivalent noise bandwidth;
- f is the equivalent focal length of the optics;

V_s is the signal voltage;
V_n is the noise voltage.

According to eq. (18), we note that calculating the value R_{ran} is conditional by calculating the terms V_s and V_n. The term V_s is a peak output voltage value of the detector. To calculate the next term V_n, we need to calculate the detector noise level, which is given by the relation [16]

$$N = (A_d \, \Delta f)^{1/2} / D^* \tag{19}$$

where
N is the noise power level;
A_d is the detector area.

Thus, the noise voltage V_n is found by

$$V_n = \sqrt{N \, R_{res}} \tag{20}$$

where R_{res} is the resistance of the detector.

The rectangular coordinates of the target x_T, y_T, and z_T can be calculated as

$$y_T = y_I \frac{R_{ran}}{f} \tag{21}$$

$$z_T = z_I \frac{R_{ran}}{f} \tag{22}$$

$$x_T = \sqrt{R_{ran}^2 - y_T^2 - z_T^2} \tag{23}$$

By calculating the rectangular coordinates of the target x_T, y_T, and z_T, we can find the spherical coordinates as

$$r_v = \sqrt{x_T^2 + y_T^2 + z_T^2} \tag{24}$$

$$\tan\eta = \frac{\sqrt{x_T^2 + y_T^2}}{z_T} \tag{25}$$

$$\tan\varphi = \frac{y_T}{x_T} \tag{26}$$

The target velocity can be calculated using the formula

$$Sp = \sqrt{SP_x^2 + SP_y^2 + SP_z^2} \tag{27}$$

where SP_x, SP_y, and SP_z are the components of the velocity on the x, y, and z axes respectively. These components can be found as

$$SP_x = \frac{\Delta x_T}{\Delta t} \tag{28}$$

$$SP_y = \frac{\Delta y_T}{\Delta t} \tag{29}$$

$$SP_z = \frac{\Delta z_T}{\Delta t} \tag{30}$$

where

$\Delta x_T = x_{T2} - x_{T1}$,

$\Delta y_T = y_{T2} - y_{T1}$,

$\Delta z_T = z_{T2} - z_{T1}$,

$\Delta t = t_2 - t_1$, where t_1 and t_2 are the time at positions 1 and 2 respectively.

Computer program was prepared to using the above model to calculate the coordinates of IR images on thermograpgic systems.

3. CASE STUDIES

3.1 Fixed Target

Consider the target appears on the entrance aperture of the system as shown in Fig. 4 with the polar coordinates (the radius a_1 and the angle z_1). The designed software engaged with the thermographic system was used to calculate the coordinates, range, and the velocity of the target. Figure 5 shows the calculated target trace. It is clear that the target velocity is zero every where.

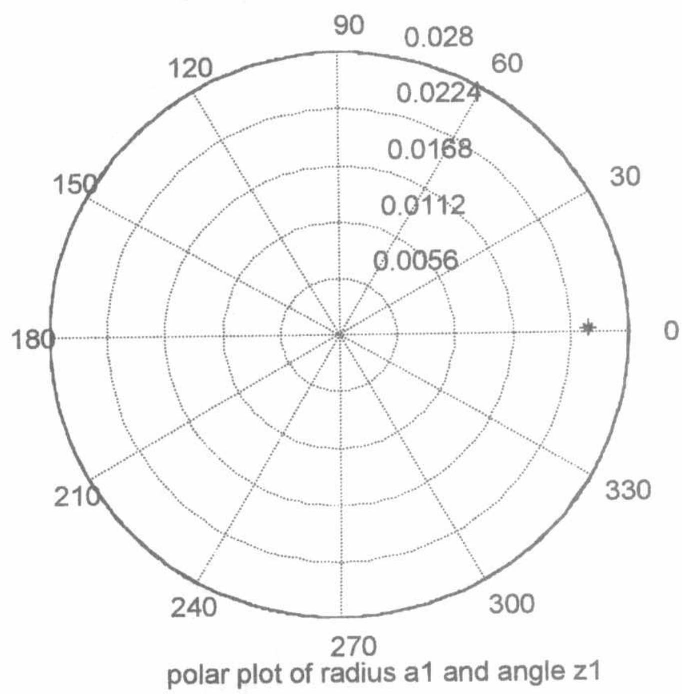

Fig. 4. The fixed target as appears on the entrance aperture (input)

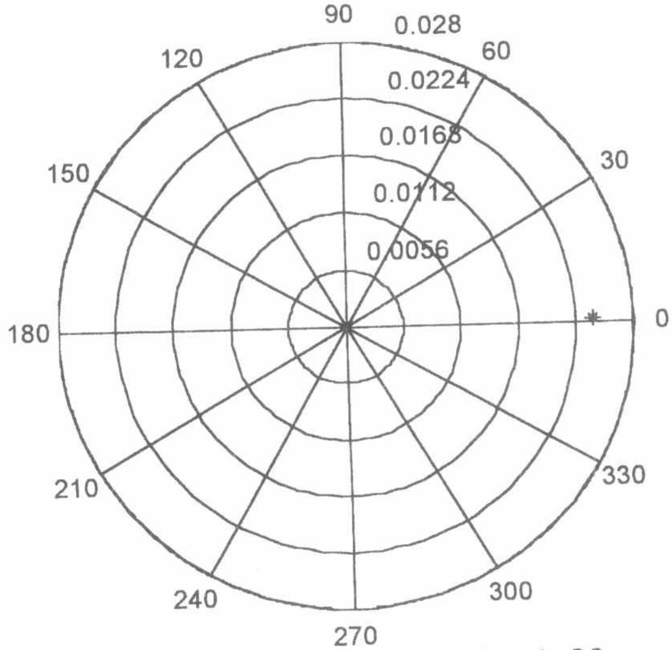

Fig. 5. The fixed target as appears on the entrance aperture (output)

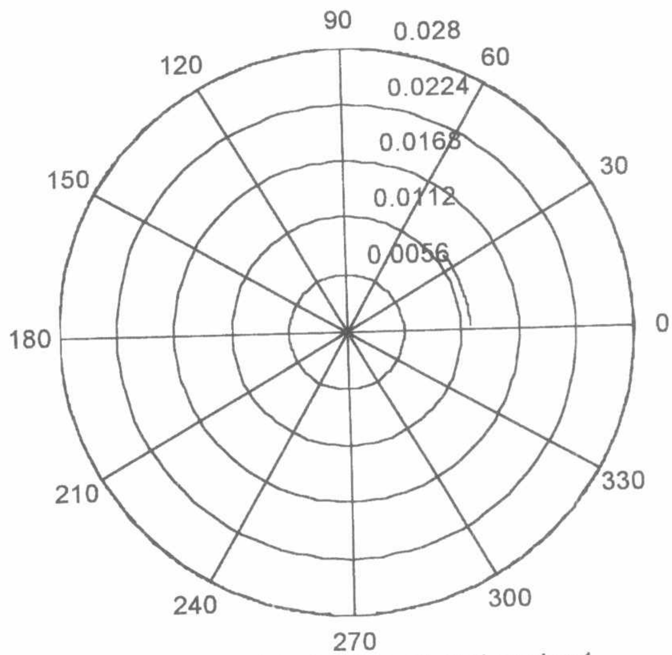

Fig. 6. Trace of the moving target with a constant velocity on the entrance aperture (input)

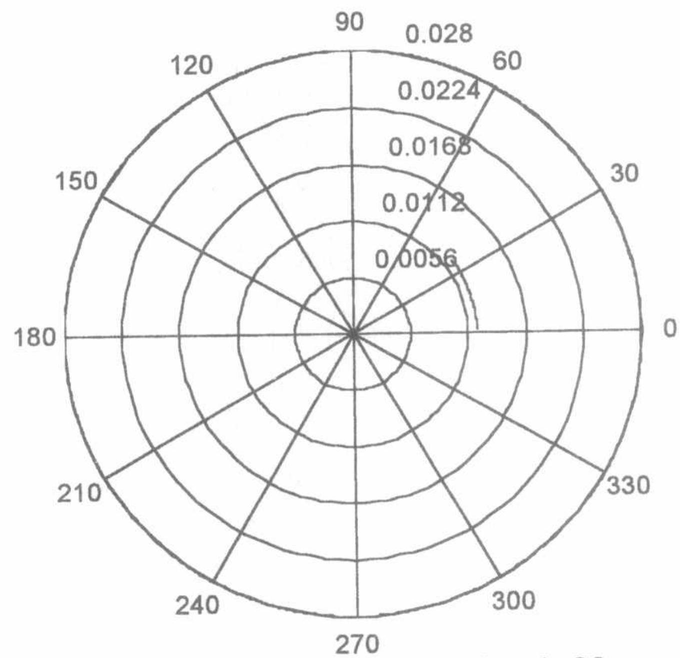

Fig. 7. The trace of the moving target with a constant velocity on the entrance aperture (output) as a results of the calculations using the designed software

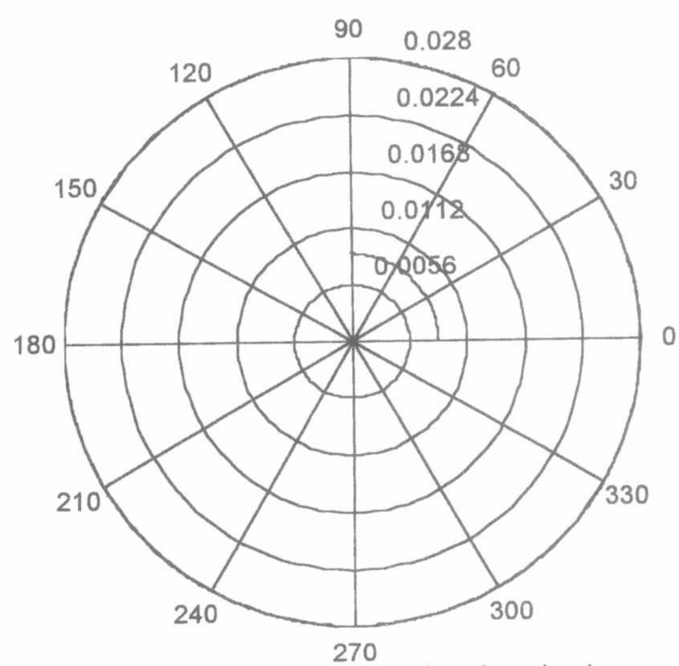

Fig. 8. The trace of the moving target with a variable velocity on the entrance aperture (input)

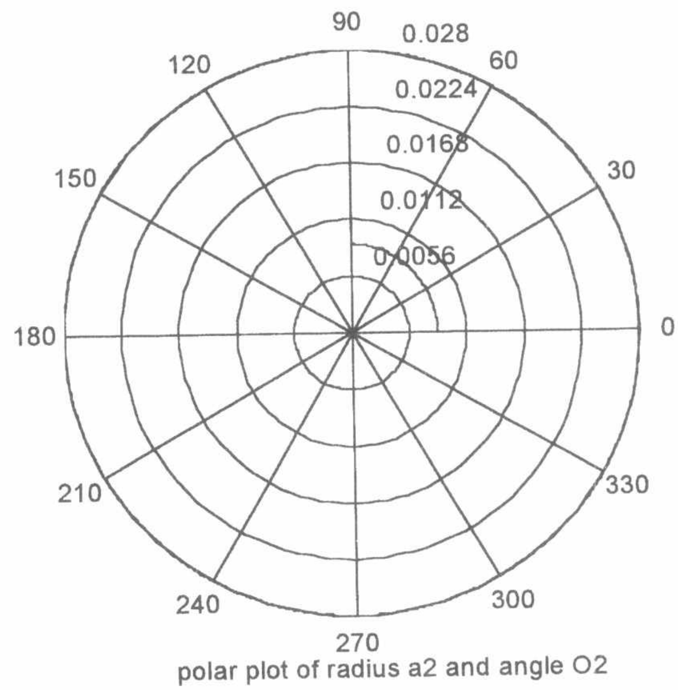

Fig. 9. The trace of the moving target with a variable velocity on the entrance aperture (output) as a result of the calculations using the designed software

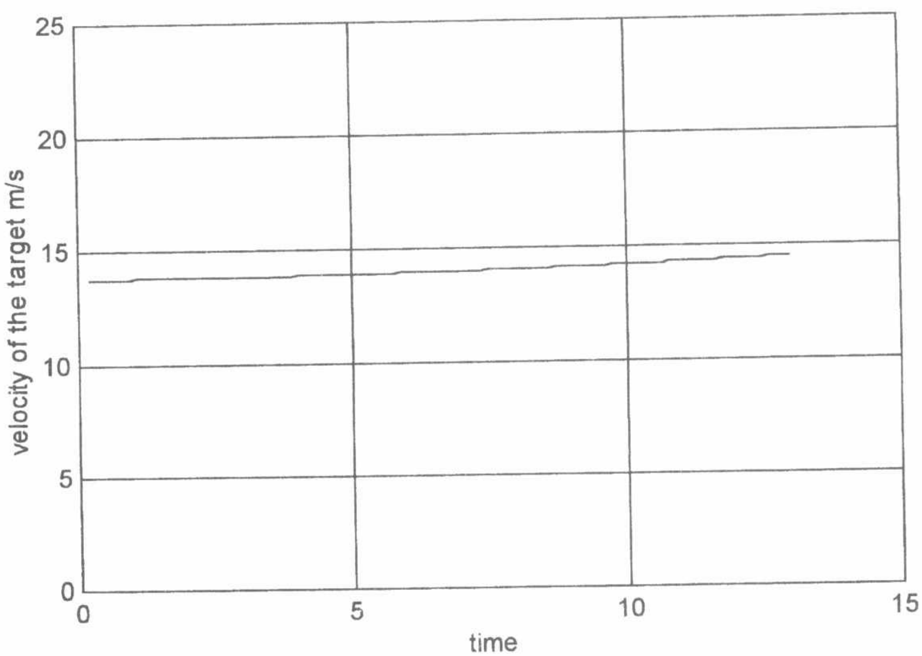

Fig. 10. The target velocity for the third case

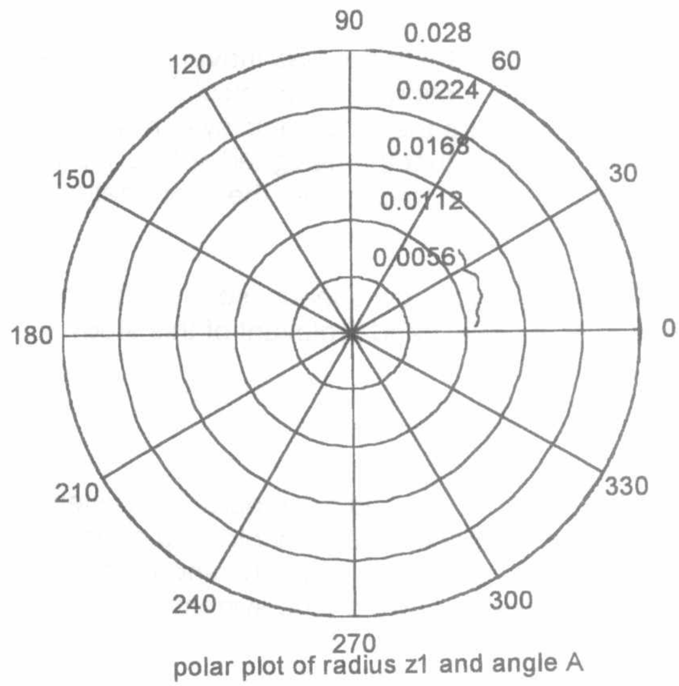

Fig. 11. The trace of random moving of the target on the entrance aperture

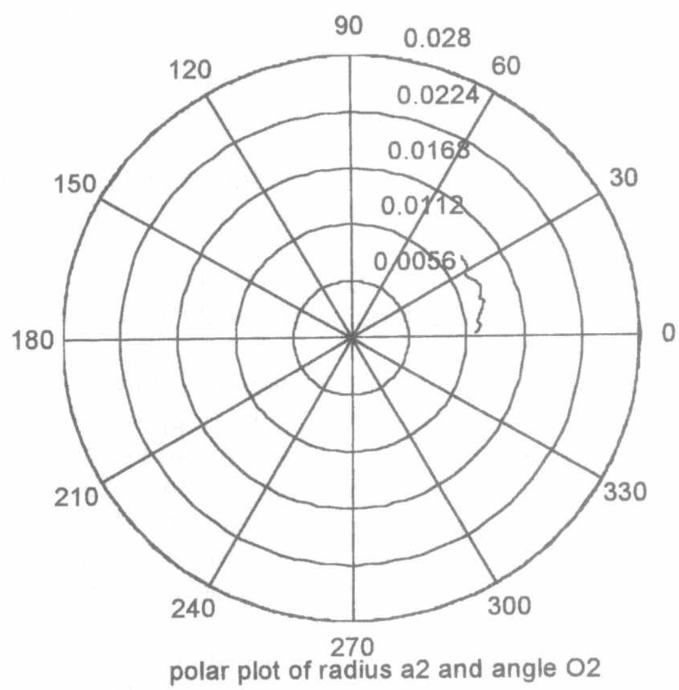

Fig. 12. The calculated trace

3.2 Moving Target

Another case study in which the target was moving with different velocities and trajectories were studied. The simulation and the calculation of these cases using the designed software engaged with the thermographic system were shown in Figs. 6, 7, 8, 9, 10, 11, and 12. It is clear that the designed software based on the previous mathematical modeling can be used to calculate the coordinates, range, and velocity of the target.

Since the situation deals with very low speeds, so the effect of noise and dynamic unstability of the target have no effect and irrelevant of this study.

4. CONCLUSION

In this paper, a design of an infrared thermographic system for positioning and coordination of targets was presented. The controlling equation and mathematical modeling was investigated by 4 case studies. The speed, coordinates and range of the targets can be determined and shown on the system display.

5. REFERENCES

[1] Gaussorgues, G., Infrared Thermography, London: Chapman and Hall, (1994).

[2] Biberman, L. B., Reticles in Electro-Optical Devices, London: Pergamon Press, (1966).

[3] Taylor, J. S., Driggers, Jr. and R. G., "Tracking with Two Frequency-Modulated Reticles." Opt. Eng., Vol. 32, No. 5, pp 1101-1104, (1993).

[4] Meads, M. M., Driggers, R. G., Halford, C. E. and Boreman, G. D., "Effect of Phasing Sector Angular Extent in FM Reticles." Appl. Opt., Vol. 31, No. 22, pp 4578-4581,(1992).

[5] Driggers, R. G., Halford, C. E. and Boreman, G. D., "Marriage of Frequency Modulation Reticles to Focal Plane Arrays." Opt. Eng., Vol. 30, No. 10, pp 1516-1521, (1991).

[6] Driggers, R. G., Halford, C. E. and Boreman, G. D., "Use of Spatial Light Modulators in Frequency Modulation Reticle Trackers." Opt. Eng., Vol. 29, No. 11, pp 1398-1403, (1990).

[7] Chao, Z. W. and Chu, J. L., "Parameter Analysis for Frequency Modulation Reticle Design." Opt. Eng., Vol. 27, No. 6, pp 443-451, (1988).

[8] Chao, Z. W. and Chu, J. L., "General Analysis of Frequency-Modulation Reticles." Opt. Eng., Vol. 27, No. 6, pp 440-442, (1988).

[9] Olsson, G., "Simulation of Reticle Seekers by Means of an Image Processing System." Opt. Eng., Vol. 33, No. 3, pp 730-736, (1994).

[10] Craubner, S., "Digital Simulation of Reticle System." Opt. Eng., Vol. 20, No. 4, pp 608-615, (1981).

[11] Driggers, R. G., Halford, C. E. and Boreman, G. D., "Parameters of Spinning AM Reticles." Appl. Opt., Vol. 30, No. 19, pp 2675-2684, (1991).

[12] Driggers, R. G., Halford, C. E., Boreman, G. D., Latman, D. and Williams, K. F. "Parameters of Spinning FM Reticles." Appl. Opt., Vol. 30, No. 7, pp 887-895, (1991).

[13] Sanders, J. S., Driggers, R. G., Halford, C. E. and Griffin, S. T., "Imaging with Frequency-Modulated Reticles." Opt. Eng., Vol. 30, No. 11, pp 1720-1724, (1991).

[14] Suzuki, K., "Analysis of Rising-Sun Reticle." Opt. Eng., Vol. 18, No. 3, pp 350-351, (1979).

[15] Hudson, R. D., Infrared System Engineering, New York: John Wiley and Sons, (1968).

[16] Seyrafi, K. and Hovanessian, S. A., Introduction to Electro-Optical Imaging and Tracking Systems, London: Artech House, (1993).